Stability of Hingeless Rotor Blades in Hover with Pitch-Link Flexibility

Dewey H. Hodges* and Robert A. Ormiston*
Ames Directorate, U.S. Army Air Mobility R&D Laboratory, Moffett Field, Calif.

A stability analysis of a single cantilevered helicopter rotor blade in hover is presented. The blade is represented by an elastic uniform beam, cantilevered in bending and having a torsional root spring to simulate pitch-link flexibility. Nonlinear equations are adapted for a linearized stability analysis about the blade equilibrium operating condition. Numerical results are obtained for hingeless rotor configurations having pitch-link flexibility, precone, droop, twist, and flap-lag structural coupling. The results indicate that hingeless rotor stability characteristics are sensitive to changes in most configuration parameters. For a given torsion frequency, the effect of pitch-link flexibility is generally found to be similar to the effect of blade torisional flexibility. Droop and precone, although physically similar, exhibit different effects on stability when pitch-link flexibility is present. Twist is shown to influence the stability by altering the flap-lag structural coupling.

Nomenclature

a = airfoil lift-curve slope, 2π per rad
b = number of blades per rotor
c = blade chord, m
c_{d_0} = airfoil profile drag coefficient
f = ratio of pitch-link stiffness to blade elastic torsion stiffness, Eq. (1)
GJ = blade elastic torsion rigidity, N-m
I = approximate rigid blade flapping moment of inertia, kg-m^2
k_A = polar area radius of gyration, m
k_{m_1}, k_{m_2} = principal mass radii of gyration, m
k_Φ = pitch-link stiffness, N – m/rad
K_β = approximate rigid blade flapping spring stiffness, N – m/rad
K_ζ = approximate rigid blade lead-lag spring stiffness, N – m/rad
K_Θ = approximate rigid blade total torsion equivalent spring stiffness, N – m/rad
K_ϕ = approximate rigid blade torsional spring stiffness, N – m/rad
K_Φ = approximate rigid blade pitch-link spring stiffness, N – m/rad
N = number of assumed mode shapes for each of the elastic torsion, flap bending, and lead-lag bending deflections
p = approximate rigid blade flap frequency, made dimensionless by Ω
R = blade length, m
$\mathfrak{R}$ = structural coupling parameter
$\bar{x}$ = radial station along blade, made dimensionless by blade length R
β_d = blade droop, positive down, rad
β_{pc} = blade precone, positive up, rad
γ = blade Lock number
ϵ = small parameter of the order of magnitude of the bending slopes
θ_t = twist parameter, twist angle = $-\theta_t \bar{x}$, rad
θ_0 = blade root pitch angle, positive, leading edge up, rad
$\theta_{3/4}$ = blade pitch angle at $\bar{x} = 3/4$ ($=\theta_0 - \frac{3}{4}\theta_t$), rad
θ_ζ = effective pitch-lag coupling
Θ = approximate rigid blade total torsion deflection, rad
σ = rotor solidity, $bc/\pi R$
σ_v = real part of lead-lag mode eigenvalue, made dimensionless by Ω
ϕ = blade torsional deflection, rad
ϕ_i = approximate rigid blade induced inflow angle, rad
Φ = blade root pitch-link torsional deflection, rad
ω_v = blade fundamental lead-lad bending frequency made dimensionless by Ω
ω_w = blade fundamental flap bending frequency, made dimensionless by Ω
ω_ϕ = blade fundamental torsion frequency, made dimensionless by Ω
Ω = blade angular velocity, rad/sec
$(\ )_0, \Delta(\ )$ = equilibrium and perturbation components of blade deflections

Introduction

THE general problem of helicopter aeroelastic stability involves coupling between the motion of the individual blades and coupling between the rotor and the body of the helicopter. The complexity of the general problem poses a considerable challenge to the analyst, both in developing an analytical model of the system and in understanding its physical behavior. An important part of the general rotor-body dynamic system is the single blade rotating about an axis fixed in space. For many problems of practical interest, blade-to-blade and rotor-body couplings are not significant, and the analysis of a single rotor blade constitutes an important problem by itself. Even when coupling with other blades and the body is significant, the single-blade behavior often remains recognizable and can be helpful in understanding the behavior of the more complete system. For this reason, the dynamics of a single blade represents an important fundamental step in the study of helicopter dynamics.

Helicopter rotors with cantilever blades are commonly termed "hingeless rotors." In contrast with the more conventional articulated rotor, the cantilever blades of the hingeless rotor are attached directly to the hub without flap or lead-lag hinges. This configuration reduces mechanical complexity and improves helicopter flying qualities by increasing rotor control power and angular rate damping. The lack of hinge articulation also alters the structural charac-

Presented at the AIAA/ASME/SAE 17th Structures, Structural Dynamics, and Materials Conference, May 5-7, 1976, King of Prussia, Pa.; submitted May 21, 1976; revision received Jan. 20, 1977.

Index categories: Helicopters; Aeroelasticity and Hydroelasticity; Structural Dynamics.

*Research Scientist. Member AIAA.

teristics of the rotor blade and can significantly influence aeroelastic stability. Aeroelastic instability is possible because of the structural coupling between bending and torsion deflections of cantilever blades. This type of instability is usually characterized by coupled flap bending, lead-lag bending, and torsion deflections, with a frequency near the lead-lag bending natural frequency.

This paper is an extension of the authors' previous work,[1] which treated a basic untwisted torsionally elastic cantilever blade with uniform radial distributions of mass and stiffness. The configuration included precone and an approximate representation of flap-lag structural coupling intended to simulate more general configuration having nonuniform radial distributions of bending stiffness. The present work includes the additional configuration parameters of twist, pitch-link flexibility, and droop. As in Ref. 1, the blade section mass center, aerodynamic center, and elastic axis are coincident, and a quasisteady aerodynamic formulation is used. The exclusion of certain details in the present research is consistent with the objective of obtaining a clear and relatively complete understanding of the fundamental behavior of the system. The addition of extraneous details at this point would complicate the analysis unnecessarily and obscure the interpretation of the results.

The derivation of the equations of motion, given in detail in Ref. 2, is briefly described. The modal solution method is outlined and results are presented in the form of stability boundaries and lead-lag mode damping. For additional background discussion of the aeroelastic stability of hingeless rotor blades, and a discussion of recent pertinent research, the reader is referred to Ref. 1.

Description of Rotor-Blade Configuration

A comprehensive study of hingeless rotor stability is a formidable task because of the many important configuration parameters. The present study is limited to a few of the main parameters. A cantilever blade structure (Fig. 1) is composed of two flexible beam segments joined by the pitch-change bearing. The inboard hub segment is fixed to the hub at the root end of the blade, whereas the outboard segment can be rotated about the pitch-change bearing by moving the pitch link vertically from the swashplate controls. Pitch-link flexibility, represented by a spring element, will permit rigid-body pitching motion of the outboard blade segment (i.e., root torsion). Certain small angular offsets of the blade axis are often provided to reduce blade-bending stresses, to improve rotorcraft flying qualities, or to enhance rotor-blade aeroelastic stability. Two of these angular offsets are considered here. Precone is the inclination of the pitch-change bearing with respect to the plane of rotation (positive upward); droop is an inclination (positive downward) of the blade segment outboard of the pitch-change bearing (as illustrated in Fig. 2).

Structural coupling between flap and lead-lag bending depends on the relative stiffness of the blade segments inboard and outboard of the pitch bearing, because the principal elastic axes of the outboard blade segment rotate through the angle θ_0 as the blade pitch angle varies, whereas the inboard segment principal axes do not. The resultant effective orientation of principal axes depends on the blade geometry and distribution of bending stiffnesses inboard and outboard of the pitch bearing. Although such variations in flap-lag structural coupling significantly influence stability, they cannot be treated exactly by the present analysis which is based on the equations of motion for a cantilever beam with uniform mass and stiffness.

In the present analysis, the inboard beam segment is eliminated and the pitch change bearing is placed in the hub. The effect of the inboard beam segment on flap-lag structural coupling can be approximately retained, however, by arbitrarily setting the inclination of the principal elastic axes of a uniform single-segment blade equal to some effective principal axis inclination of the nonuniform blade. This is accomplished by having the uniform blade structural principal axes inclined at some fraction $\Re\theta_0$ of the blade pitch angle θ_0 while the mass and inertial terms are unchanged. The factor $\Re$ is called the structural coupling parameter. When $\Re = 1$, the original equations are retained, but as $\Re$ is reduced to zero, the flap-lag structural coupling terms diminish and eventually vanish. Although this is only an approximation of the true effect of flap-lag structural coupling, it greatly simplifies the equations and does illustrate the type of behavior that would be expected for a general nonuniform blade.

Although some analyses[2,4] have treated torsionally rigid rotor blades with pitch-link flexibility (also called root torsion), the present work includes the effects of blade torsional flexibility and pitch-link flexibility simultaneously. Reference 4 also treated both, but only included numerical results for root torsion. The parameter f defines the distribution of torsion flexibility between the pitch link and the blade

$$f = k_\Phi R/GJ \tag{1}$$

where R is the blade length and k_Φ and GJ are spring and blade torsion stiffnesses, respectively. Thus, for a given torsion frequency, $f=0$ is pure root torsion and $f=\infty$ is pure elastic torsion.

where R is the blade length and k_Φ and GJ are spring and blade torsion stiffnesses, respectively. Thus, for a given torsion frequency, $f=0$ is pure root torsion and $f=\infty$ is pure elastic torsion

Other configuration parameters of interest are the bending frequencies ω_v and ω_w, torsion frequency ω_ϕ, Lock number γ, solidity σ, dimensionless blade chord c/R, ratio of blade profile drag to the lift-curve slope c_{d_0}/a, dimensionless polar area radius of gyration k_A/R, and dimensionless principal mass radii of gyration k_{m_1}/R and k_{m_2}/R. These parameters are defined in Ref. 1. All results presented here are for configurations with $\omega_w = 1.15$, $\gamma = 5$, $\sigma = 0.1$, $c/R = \pi/40$, $c_{d_0}/a = 0.01/2\pi$, $k_A/k_{m_2} = (1.5)^{1/2}$, $k_{m_1}/R = 0$, and $k_{m_2}/R = 0.025$. The remaining parameters ω_v, ω_ϕ, $\Re$, f, β_d, β_{pc}, θ_t, and θ_0 (or $\theta_{3/4} = \theta_0 - \frac{3}{4}\theta_t$) are specified in the captions of each figure.

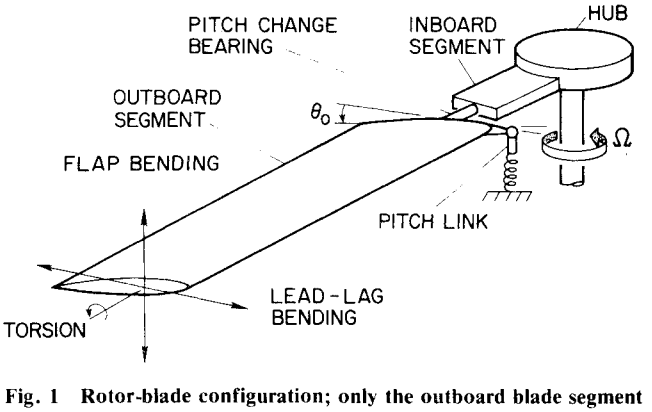

Fig. 1 Rotor-blade configuration; only the outboard blade segment is included in the present analysis.

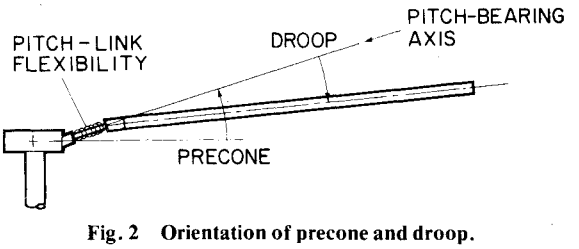

Fig. 2 Orientation of precone and droop.

Description of the Analysis

The equations of motion for the blade are derived in Ref. 2. The structural terms are adapted from Ref. 5 and the inertial terms are obtained from the kinetic energy. The aerodynamic terms are developed from strip theory based on a quasisteady approximation of Greenberg's two-dimensional unsteady airfoil theory.[6] Uniform induced inflow is assumed based on the momentum theory approximation at the ¾-blade radius. The total blade pitch angle in calculating the inflow is taken to be $\theta_0 - \theta_t \bar{x} + \Phi_0 + \phi_0(\bar{x})$ at $\bar{x} = \frac{3}{4}$. The derivation of aerodynamic forces is slightly different from Ref. 1: a) no small-angle assumptions are made for θ_0, the blade pitch angle at the root, and b) the apparent mass terms in the blade-torsion equation due to blade coning are retained in this analysis.[2] The equations of motion are nonlinear, and nonlinear terms are retained up through second order in ϵ, where ϵ is of the order of magnitude of the bending slopes. Third-order terms are retained in the Φ equation to achieve torsion moment equilibrium between the blade elastic torsion moment and the pitch-link spring moment at the blade root at high pitch angles. The corresponding third-order terms involving Φ in the flap, lead-lag, and torsion equations are retained so that the mass and stiffness matrices will be symmetric and the gyroscopic matrix will be antisymmetric (*in vacuo*). The equations of motion are hybrid. There are three integro-partial differential equations for elastic lead-lag and flap bending and elastic torsion, v, w, and ϕ, respectively, and one integro-differential equation for the root torsion angle Φ.

Both pitch-link flexibility and blade torsional flexibility affect the uncoupled ($\theta_0 = \theta_t = \beta_d = \beta_{pc} = 0$) fundamental torsion natural frequency of a uniform blade rotating in a vacuum.[2] Thus, when we examine blade configurations with a given torsion frequency ω_ϕ, a change in f will affect both GJ and k_Φ in order to keep ω_ϕ constant.

Standard mode shapes for a nonrotating uniform cantilever beam are used in the application of Galerkin's method to reduce the four hybrid equations to $3N+1$ nonlinear ordinary differential equations. Here N is defined as the number of modes for each of the elastic torsion, flap bending, and lead-lag bending deflections. These nonlinear ordinary differential equations are linearized from small perturbation motions about the equilibrium operating condition resulting in $3N+1$ nonlinear algebraic equations for the equilibrium generalized coordinates and $3N+1$ linear ordinary differential equations with the low-frequency modes are suitably converged and a coordinates. The linear perturbation equations have coefficients that depend on the equilibrium generalized coordinates and yield a standard eigenvalue problem

$$\{\dot{X}\} = [P]\{X\} \tag{2}$$

where $[P]$ is a $(6N+2) \times (6N+2)$ matrix. Since cantilever blade torsion modes do not satisfy the moment equilibrium at the blade root when the pitch link is flexible, the results are sensitive to N. For $N=5$, however, the eigenvalues associated with the low-frequency modes are suitably converged and a modal analysis is used that reduces the eigenvalue problem from 32×32 to only 12×12. As pointed out in Ref. 1, this is equivalent to using six fully coupled mode shapes associated with the eigenvalues of the lowest frequency modes. After the truncation from 32 degrees of freedom to 12, the modes remaining are two or three lead-lag modes, two or three flap modes, and one torsion mode, depending on the values of ω_v, ω_w, and ω_ϕ. This greatly reduces the size of the eigenvalue problem while leaving the eigenvalues for the low-frequency modes virtually unchanged. The nonlinear algebraic equilibrium equations are solved by Brown's method,[7] and the eigenvalue problem is solved by the QR algorithm.

Results

Before discussing the present results, it will be useful to briefly describe the effects of basic configuration variables on hingeless rotor-blade stability.[1] For cantilever rotor blades without chordwise offsets between the center of mass, elastic axis, and aerodynamic center, the stability characteristics are mainly determined by two structural effects: flap-lag structural coupling and bending-torsion structural coupling. The former couples flap bending and lead-lag bending motions when the flap and lead-lag bending stiffnesses are unequal and when the principal elastic axes are inclined to the plane of rotation. Normally, this inclination is a function of the pitch angle of the rotor blade. As discussed previously, it also depends on the relative stiffness of the blade segments inboard and outboard of the pitch bearing, which is arbitrarily simulated by the parameter $\Re$. For soft inplane configurations, $\omega_v < 1.0$, flap-lag structural coupling stabilizes the blade motion, i.e., it increases the damping of the lead-lag mode. For stiff inplane configurations, $\omega_v > 1.0$, flap-lag structural coupling effects are larger and more varied. Small coupling can produce lead-lag mode instabilities while large coupling is usually highly stabilizing. If the flap and lead-lag stiffnesses are equal, the configuration is called "matched stiffness" and flap-lag structural coupling is eliminated.

The bending-torsion structural coupling is generally more complicated and can have a more substantial influence on blade motion stability than flap-lag structural coupling. This coupling occurs when torsional moments are generated by simultaneous flap and lead-lag bending of blade configurations having unequal flap and lead-lag bending stiffnesses. The resulting torsional deflections are proportional to the torsional flexibility of the blade. This coupling is

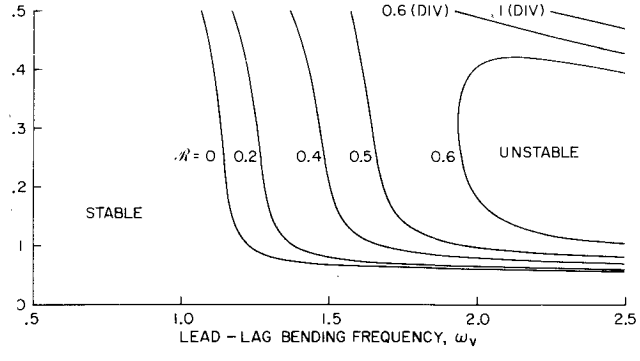

Fig. 3 Effect of flap-lag structural coupling on stability boundaries of pitch angle vs lead-lag frequency for a blade without pitch-link flexibility, droop, precone, or twist; $\omega_\phi = 5$.

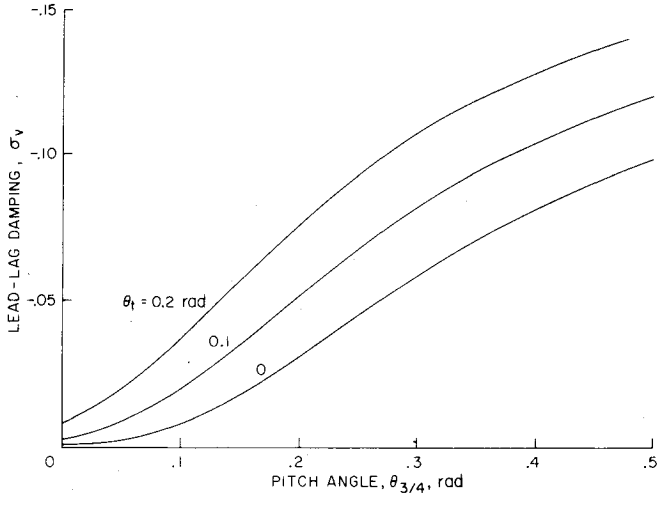

Fig. 4 Effect of twist on lead-lag damping vs blade pitch angle; $\omega_v = 1.5$, $\Re = 1.0$, $\omega_\phi = 5$, $f = \infty$, $\beta_d = \beta_{pc} = 0$.

inherently nonlinear, since it depends on the product of bending deflections, but for small-perturbation motions about an equilibrium operating condition, it can be characterized by linear coefficients that depend on the equilibrium bending deflections. These coefficients relate the blade pitch motion to flap and lead-lag bending and are termed "pitch-flap" and "pitch-lag" couplings, respectively. Precone strongly influences pitch-lag coupling, since it influences the equilibrium flap deflection of the blade. These couplings vanish for the matched stiffness configuration.

For configurations with very low torsion frequency, the stability behavior is complex and is dominated by torsional dynamics. For higher torsional frequencies, $\omega_\phi \gtrsim 5$, the effects of torsional dynamics are less important and the effects of torsion frequency and precone are readily understood in terms of their influence on the effective pitch-flap and pitch-lag coupling parameters. The influence of these coupling parameters on stability of torsionally rigid blades is reasonably well understood.[8,9] For soft inplane configurations without precone, negative pitch-lag coupling is produced for positive equilibrium flap deflections and stabilizes the lead-lag mode for all values of flap-lag structural coupling. Precone reverses the sign of the pitch-lag coupling at low blade pitch angles and can produce lead-lag mode instability, sometimes termed "precone instability." The effect of pitch-lag coupling on stiff inplane configurations depends strongly on the degree of flap-lag structural coupling. When the flap-lag coupling is low, torsional flexibility produces destabilizing negative pitch-lag coupling, but this coupling is stabilizing for configurations with high flap-lag structural coupling. Precone is destabilizing when the flap-lag structural coupling is high but stabilizing when it is low. The effects of the new configuration variables introduced here can be roughly interpreted in the context of this brief background discussion.

Flap-Lag Structural Coupling

Figure 3 shows the effect of $\Re$ on the stability boundaries of pitch angle vs lead-lag frequency for a typical torsional frequency. The blade is torsionally flexible, and there is no pitch-link flexibility, precone, droop, or twist. The stability boundaries denote lead-lag mode instabilities, except that the notation "DIV" on a boundary refers to a flap mode divergence. The results show that stiff inplane configurations will be unstable for low values of $\Re$ and stable for large $\Re$. In practical configurations, a value of $\Re = 0$ is not likely because this implies that all bending flexibility is inboard of the pitch-change bearing. It represents only an ideal limiting case of a rotor-blade configuration. (Results for the blade configuration in Fig. 3 were given previously[1] with some small quantitative differences in the stability boundary locations. This resulted from the addition of a small apparent mass aerodynamic pitching moment term to the present results.)

Twist

The effect of blade twist is to introduce an increment of flap-lag structural coupling that varies along the blade and is independent of blade pitch angle. Twist also influences the distribution of aerodynamic forces along the blade, but this generally has a small effect on stability. When blade twist is included in the configuration, the use of the structural coupling parameter $\Re$ becomes ambiguous. For example, $\Re = 0$ implies that the bending flexibility of the blade outboard of the pitch bearing is zero, in which case twist could have no significance in a structural sense. Therefore, it is advisable to eliminate $\Re$ from the equations, which effectively means $\Re = 1.0$. This restores the equations to their original form given in Ref. 4. As noted in Fig. 3, the configuration $\Re = 1.0$ does not exhibit significant unstable behavior, so the effects of twist will be observed as they influence lead-lag mode damping. Results for a stiff inplane configuration, $\omega_v = 1.5$, are shown in Fig. 4. For a given value of the blade pitch angle at the ¾-radius, twist increases the inclination of the principal flexural axes of the blade cross section at the root end of the blade. This increases flap-lag structural coupling in the region of the blade where most of the bending takes place. For the stable stiff inplane configuration shown, this increased coupling increases the lead-lag damping by a significant amount, particularly at low blade pitch angles. The effect of twist would be less important for soft inplane configurations since the difference between flap and lead-lag bending stiffnesses is smaller.

Pitch-Link Flexibility

The effect of the distribution of torsion flexibility between flexible pitch-link motion and blade elastic torsion is illustrated in the next series of figures. The parameter f represents the ratio of blade pitch-link stiffness to the blade torsional rigidity. A value of infinity corresponds to the configurations without pitch-link flexibility treated in Ref. 1 and a value of zero corresponds to a torsionally rigid blade with rigid-body pitching motion at the pitch bearing. At any given torsion frequency, the main effect of the distribution of flexibility is to modify the torsion mode shape. It is not anticipated that this will produce a fundamental change in the stability of typical configurations without droop. For these results, the structural coupling parameter $\Re$ was chosen to be zero to illustrate the effects of f on typical stability boundaries. The first result in Fig. 5 shows the effect of f on the stability boundaries of pitch angle vs lead-lag frequency for a torsion frequency $\omega_\phi = 8$. Twist, precone, and droop are all zero. The effect of adding pitch-link flexibility (f decreasing from ∞ to 0) is to slightly destabilize the stiff inplane instability; i.e., the instability occurs at a lower blade pitch angle. This can be attributed to the fact that the torsional flexibility is concentrated at the root of the blade where the structural torsion moments due to bending are largest. This would amplify the torsional response compared to the case where the torsional flexibility was distributed along the blade in a region of reduced structural torsion moments. This would effectively increase the influence of bending-torsion structural coupling and the associated pitch-lag coupling that is destabilizing for this configuration. Another result is given in Fig. 6 for a torsion frequency of 5; the results are similar except that, for small values of f, the stiff inplane instabilities are eliminated for a small range of θ_0 at high blade pitch angles. The lead-lag instability encountered at low pitch angle becomes stable as θ_0 is increases, but at the upper boundary a flap mode divergence occurs. For a blade without pitch-link flexibility, $f = \infty$, a high pitch angle flap divergence is present only for values of $\Re$ near 1.[1] The present results indicate that with large pitch-link flexibility, $f \cong 0$, this flap mode divergence occurs for small as well as large values of $\Re$.

The relationship of the stability boundaries to the torsional flexibility distribution and torsion frequency is shown in more details in Figs. 7 and 8. These results, for lead-lag frequencies of 1.5 and 1.1, respectively, show the stability boundaries of

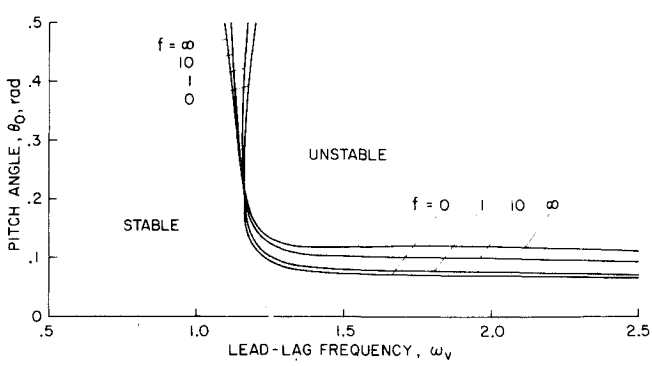

Fig. 5 Effect of relative pitch-link flexibility on stability boundaries of pitch angle vs lead-lag frequency; $\Re = 0$, $\omega_\phi = 8$, $\theta_t = \beta_d = \beta_{pc} = 0$.

θ_0 vs torsion frequency. In Fig. 7, a typical stiff inplane configuration (except for the idealization of zero flap-lag structural coupling $\Re = 0$) illustrates the stabilizing influence of increasing torsional stiffness on the low pitch angle, lead-lag mode instability. This is due to the reduction in effective pitch-lag coupling produces by bending-torsion structural coupling as the torsional stiffness becomes large. As noted earlier, the effect of pitch-link flexibility is to reduce the pitch angle at which the lead-lag mode instability occurs. For configurations with large pitch-link flexibility, the lead-lag mode instability is eliminated at high pitch angles and a flap mode divergence occurs as noted previously. Figure 7 shows that this behavior occurs only for low and moderate values of the torsion frequency. Figure 8 illustrates the complex behavior that occurs for lead-lag frequencies slightly greater than 1.0 – the region where the stiff inplane stability boundaries rapidly increase with decreasing lead-lag frequency. Although lead-lag frequencies this close to 1.0 do not represent practical configuration values because of excessive rotor-blade response to 1/rev periodic excitations, they do provide a sensitive test for aeroelastic stability analyses. Figure 8 shows that the effect of pitch-link flexibility does not change the basic character of the stability boundaries except at very low torsion frequencies; otherwise, for intermediate torsion frequencies, the high pitch angle instability changes from a lead-lag mode instability to a flap mode divergence as the relative pitch-link flexibility increases. At high torsion frequencies, the instability becomes a pure flap-lag instability.

The results for a configuration similar to that in Fig. 8 for $f = \infty$ were given previously in the discussion of Ref. 3 by Ormiston and Hodges. These results were compared to similar results for $f = 0$ given in Ref. 3. At low to moderate torsion frequencies, the two results were qualitatively different; the results from Ref. 3 for $f = 0$ did not exhibit the instability present for $f = \infty$. The difference did not appear to be due to the minor differences between torsion mode shapes for $f = 0$ and ∞. The present results in Fig. 8 for f varying continuously from 0 to ∞ indicate that the stability does not appear to be strongly dependent on f and that instability can occur at low torsion frequencies for $f = 0$.

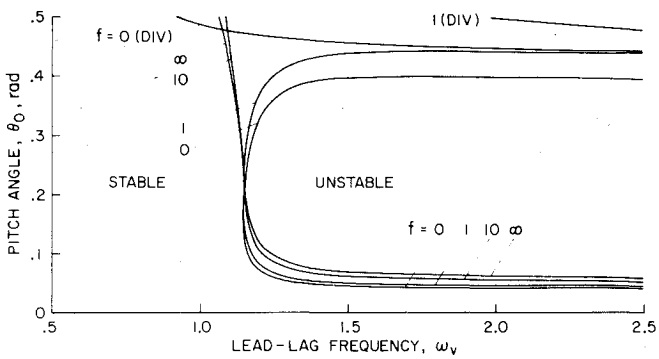

Fig. 6 Effect of relative pitch-link flexibility and blade torsion flexibility on stability boundaries of pitch angle vs lead-lag frequency; $\Re = 0$, $\omega_\phi = 5$, $\theta_t = \beta_d = \beta_{pc} = 0$.

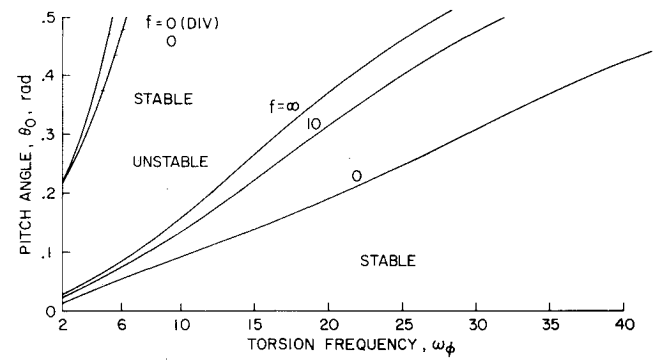

Fig. 7 Effect of relative pitch-link flexibility and blade torsion flexibility on stability boundaries of pitch angle vs torsion frequency; $\Re = 0$, $\omega_v = 1.5$, $\theta_t = \beta_d = \beta_{pc} = 0$.

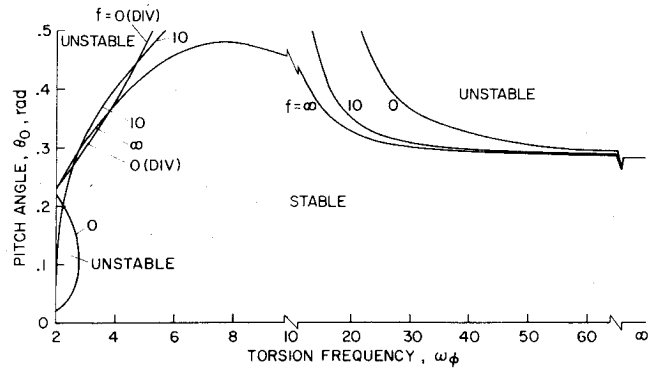

Fig. 8 Effect of relative pitch-link flexibility and blade torsion flexibility on stability boundaries of pitch angle vs torsion frequency; $\Re = 0$, $\omega_v = 1.1$, $\theta_t = \beta_d = \beta_{pc} = 0$.

As noted earlier, the effect of pitch-link flexibility is a relatively small mode-shape influence for configurations without droop. When droop is present, however, the effect of pitch-link flexibility is qualitatively different from that of elastic blade torsional flexibility.

Droop and Precone

Droop and precone are known to have a strong influence on the stability of torsionally flexible cantilever rotor blades, particularly when pitch-link flexibility is present. These effects are complex, however, and few results have been published to clarify the stability behavior for a reasonably typical blade configuration. The present analysis offers the possibility of explaining some of the interrelated effects of droop, precone, torsional frequency, and the distribution of torsional flexibility f. Reference 1 presents an extensive investigation of the effects of precone for configurations without pitch-link flexibility, and the primary structural effects were characterized in terms of the effective pitch-lag coupling of the blade. This approach can be extended to include the effects of droop and pitch-link flexibility. The previous development of the effective pitch-lag coupling used the fundamental mode perturbation equations of the elastic blade. The development of simple expressions for the equivalent pitch-lag coupling, including the new parameters, is greatly facilitated by using a simple discretized representation of the elastic blade rather than the modal perturbation equations. The derivation in the Appendix gives the following result for the effective pitch-lag coupling of the blade

$$\theta_\zeta \cong \frac{1}{K_\Theta}\left\{-\frac{\gamma}{8p^2}(K_\zeta - K_\beta)(\theta_0 - \phi_i) + \frac{(K_\zeta - K_\beta)\beta_{pc}}{p^2} - \beta_d\left[\frac{K_\zeta - K_\beta}{p^2} - \frac{K_\zeta}{1+f}\right]\right\} \tag{3}$$

This expression, although only an approximation to the actual structural behavior of an elastic blade, clearly and simply illustrates the role of each of the primary configuration variables of interest. The first two terms are due to blade pitch angle and precone. They were given in Ref. 1 in slightly different form, however, since that derivation was based on the elastic blade modal equations. Equation (3) shows that, without precone or droop, a negative pitch-lag coupling is generated for positive blade pitch angles. This is proportional to the difference between the lead-lag and flap bending stiffnesses and inversely proportional to the torsional stiffness. A similar term of opposite sign is generated by precone. This term dominates the pitch-lag coupling at low

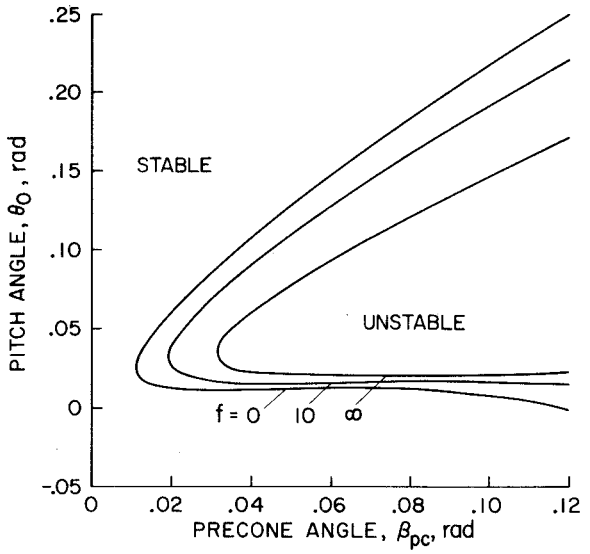

Fig. 9 Effect of relative pitch-link flexibility and blade torsion flexibility on stability boundaries of pitch angle vs precone; $\Re = 1$, $\omega_v = 1.3$, $\omega_\phi = 4$, $\theta_t = \beta_d = 0$.

angles and is responsible for the low pitch angle "precone instability." Neither blade pitch nor precone generate pitch-lag coupling for matched stiffness configurations since $K_\zeta = K_\beta$. This explains the virtual absence of instabilities for matched stiffness, uniform cantilever blades without droop.[1,8] Note, however, that, contrary to this reasoning, the results in Ref. 4 exhibited unexplained matched stiffness instabilities.

The third term for the effect of droop is more complex than the first two. Since droop influences the equilibrium flap deflection of the blade outboard of the pitch bearing, it creates a different pitch-lag coupling effect for pitch-link flexibility than for blade torsional flexibility. Thus the influence of droop in pitch-lag coupling is a function of f. There are two droop terms in Eq. (3), one similar to the precone term and one that depends only on the lead-lag bending stiffness and the distribution of torsional flexibility f. The latter term vanishes for $f = \infty$ when the pitch link is rigid and the effect of droop is identical to negative precone; it is maximized for $f = 0$ when the blade is torsionally rigid. Note

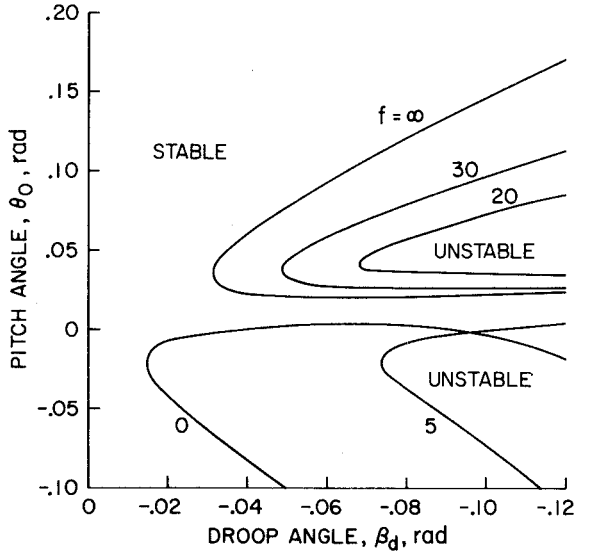

Fig. 10 Effect of relative pitch-link flexibility and blade torsion flexibility on stability boundaries of pitch angle vs droop; $\Re = 1$, $\omega_v = 1.3$, $\omega_\phi = 4$, $\theta_t = \beta_{pc} = 0$.

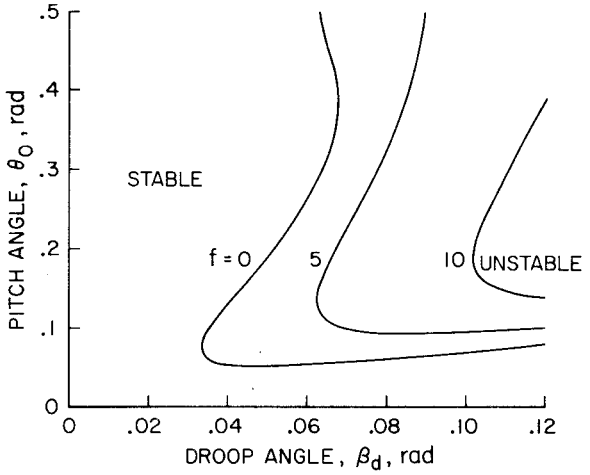

Fig. 11 Effect of relative pitch-link flexibility and blade torsion flexibility on stability boundaries of pitch angle vs droop; $\Re = 1$, $\omega_\phi = 4$, $\omega_v = 0.5697$, $\theta_t = \beta_{pc} = 0$.

that this term generates pitch-lag coupling for matched stiffness blade configurations having pitch-link flexibility and therefore can result in lead-lag mode instabilities when $\beta_d > 0$.

A few results illustrating the effects of droop and precone are given in the following figures. Figure 9 shows the effect of the torsional flexibility distribution on the precone instability that occurs at low pitch angles for both soft and stiff inplane configurations with large flap-lag structural coupling $\Re = 1.0$. A stiff inplane configuration with a torsion frequency of 4 is chosen. The effect of pitch-link flexibility is relatively small as it does not change the basic character of the stability boundary. Increasing the pitch-link flexibility increases the effective pitch-lag coupling by influencing the torsion mode shape (as noted above). The region of instability is correspondingly enlarged.

Figure 10 shows an analogous result for the same configuration but with negative droop substituted for precone. As was evident from the effective pitch-lag coupling relation [Eq.(3)], precone and negative droop have the same influence when the pitch link is rigid and the stability boundaries for $f = \infty$ are virtually identical in Figs. 9 and 10. However, as pitch-link flexibility is introduced, there is a fundamental change in the pitch-lag coupling. The contribution due to droop decreases with f and the low pitch angle instability is eliminated. For very low values of f, the sign of the pitch-lag coupling due to droop will change, and this results in instability at negative blade pitch angle.

The final result in Fig. 11 illustrates that droop and pitch-link flexibility together can cause instability for a matched stiffness configuration. While the instabilities for the stiff inplane configuration (Fig. 10) were generated by negative

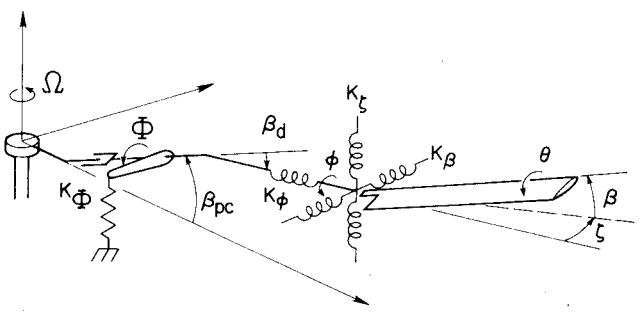

Fig. 12 Discretized representation of elastic cantilever blade showing spring elements used to develop approximate expression for effective pitch-lag coupling; spring elements are shown radially offset from center of rotation for clarity.

droop, the matched stiffness configuration requires positive droop to generate the destabilizing positive pitch-lag coupling. For the matched stiffness configuration with nonzero droop, the pitch-lag coupling due to droop depends strongly on f and the coupling decreases to zero as f increases to ∞. This is clearly evident in Fig. 11 as the region of instability becomes smaller as the pitch link becomes stiffer.

Conclusions

The present results are intended to give some insight into the effects of certain configuration parameters on the general stability characteristics of hingeless rotor blades. The main results are summarized as follows:

1) The effects of flap-lag structural coupling significantly influence the stability characteristics of torsionally flexible hingeless rotor blades. Typical lead-lag mode instabilities that occur for stiff inplane configurations are generally stabilized by increased flap-lag structural coupling.

2) Blade twist increases flap-lag structural coupling and may significantly increase lead-lag mode damping, particularly for stiff inplane configurations.

3) Pitch-link flexibility moderately influences rotor-blade stability, primarily by altering the torsion mode shape and increasing the effective pitch-lag coupling. Although there are some exceptions, the basic character of the stability boundaries is relatively insensitive to the distribution of torsional flexibility between the pitch link and the blade.

4) Blade droop and pitch-link flexibility together can strongly influence blade stability. Without pitch-link flexibility, the effect of negative droop is equivalent to precone. With pitch-link flexibility, droop produces additional effects that can generate instability in matched stiffness blade configurations and strongly influence other configurations as well.

Appendix

The derivation of the effective structural pitch-lag coupling of a discretized cantilever blade is given here. The pitch-link stiffness and blade torsional rigidity are lumped into the springs K_Φ and K_ϕ, respectively. The orientation of these springs is determined by the precone and droop of the blade. The flap and lead-lag stiffnesses are represented by the orthogonal springs K_β and K_ζ, respectively. Flap-lag structural coupling is ignored by fixing the orientation of the K_β and K_ζ springs independent of the blade pitch angle θ_0. Using small-angle approximations, the structural equilibrium of the spring system yields the following expression for the total torsional deflection of the blade, where $\Theta \cong \Phi + \phi$

$$\Theta \cong -\frac{1}{K_\Theta}\left[(K_\zeta - K_\beta)\beta\zeta - \frac{K_\zeta \beta_d \zeta}{1+f}\right] \tag{A1}$$

where

$$f = K_\Phi / K_\phi \qquad K_\Theta = K_\phi K_\Phi / (K_\phi + K_\Phi)$$

The first term in this expression is the primary bending-torsion structural coupling effect and it is nonlinear in the blade bending deflections β and ζ. Its contribution to linear stability is readily obtained by considering small-perturbation motions $(\Delta\beta, \Delta\zeta, \Delta\Theta)$ about a known equilibrium condition $(\beta_0, \zeta_0, \Theta_0)$. By ignoring nonlinear terms in the perturbation quantities, the ratio of perturbation blade-pitch deflection to perturbation lead-lag deflection, which is the effective pitch-lag coupling, becomes

$$\theta_\zeta \equiv \frac{\Delta\Theta}{\Delta\zeta} = -\frac{1}{K_\Theta}\left[(K_\zeta - K_\beta)\beta_0 - \frac{K_\zeta \beta_d}{1+f}\right] \tag{A2}$$

The equilibrium flapping deflection of the blade may be approximated by considering the aerodynamic and inertial moments acting on the blade[8] and again neglecting flap-lag coupling.

$$\beta_0 = \frac{\gamma}{8p^2}(\theta_0 - \phi_i) - \frac{\beta_{pc} - \beta_d}{p^2} \tag{A3}$$

where

$$\gamma = \rho a c R^4 / I; \qquad p = \sqrt{1 + K_\beta / I\Omega^2}$$

Note that $(\theta_0 - \phi_i)$ is the blade pitch angle minus the induced inflow angle due to rotor downwash. It is the angle of attack of the blade in equilibrium conditions. Substituting Eq. (A3) into (A2) yields, for the effective pitch-lag coupling

$$\theta_\zeta = \frac{1}{K_\Theta}\left\{-\frac{\gamma}{8p^2}(K_\zeta - K_\beta)(\theta_0 - \phi_i) + \frac{(K_\zeta - K_\beta)\beta_{pc}}{p^2} - \beta_d\left[\frac{K_\zeta - K_\beta}{p^2} - \frac{K_\zeta}{1+f}\right]\right\} \tag{A4}$$

References

[1] Hodges, D.H. and Ormiston, R.A., "Stability of Elastic Bending and Torsion of Uniform Cantilever Rotor Blades in Hover and Variable Structural Coupling," NASA TN D-8192, April 1976.

[2] Hodges, D.H., "Nonlinear Equations of Motion for Cantilever Rotor Blades in Hover with Pitch-Link Flexibility, Twist, Precone, Droop, Sweep, Torque Offset, and Blade Root Offest," NASA TM X-73,112, May 1976.

[3] Friedmann, P., "Some Conclusions Regarding the Aeroelastic Stability of Hingeless Helicopter Blades in Hover and Forward Flight," *Journal of the American Helicopter Society,* Vol. 18, Oct. 1973, pp. 13-23; (discussion by R.A. Ormiston and D.H. Hodges, Vol. 20, July 1975, pp. 46, 47).

[4] Friedmann, P., "Influence of Structural Damping, Preconing, Offsets and Large Deflections on the Flap-Lag-Torsional Stability of a Cantilevered Rotor Blade," *AIAA Journal,* Vol. 15, Feb. 1977, pp. 149-158.

[5] Hodges, D.H. and Dowell, E.H., "Nonlinear Equations of Motion for the Elastic Bending and Torsion of Twisted Nonuniform Rotor Blades," NASA TN D-7818, Dec. 1974.

[6] Greenberg, J.M., "Airfoil in Sinusoidal Motion in a Pulsating Stream," NASA TN 1326, June 1947.

[7] Brown, K.M., "A Quadratically Convergent Newton-Like Method Based Upon Gaussian Elimination," *SIAM Journal on Numerical Analysis,* Vol. 6, April 1969, pp. 560-569.

[8] Ormiston, R.A. and Hodges, D.H., "Linear Flap-Lag Dynamics of Hingeless Helicopter Rotor Blades in Hover," *Journal of the American Helicopter Society,* Vol. 17, April 1972, pp. 2-14.

[9] Peters, D.A., "An Approximate Closed-Form Solution for Lead-Lag Damping of Rotor Blades in Hover," NASA TM X-62,425, April 1975.